

DOI: 10.24425/amm.2021.134763

M. TOMASZEWSKA¹, J. DZIK^{1*}, B. WODECKA-DUŚ¹, T. PIKULA²,
M. ADAMCZYK-HABRAJSKA¹, D. SZALBOT¹, D. CHOCYK³

THE EFFECT OF Ho DOPING CONTENTS ON THE STRUCTURAL, MICROSTRUCTURE AND DIELECTRIC PROPERTIES OF Bi₅Ti₃FeO₁₅ AURIVILLIUS CERAMICS

Aurivillius Bi_{5-x}Ho_xTi₃FeO₁₅ (BHTFO) multiferroic ceramics with different holmium doping contents were synthesized by conventional solid state reaction. The effect of holmium doping on the microstructure, structural and dielectric behaviors of BHTFO ceramics were investigated in details. Microstructure and crystalline structure studies of ceramics were carried out at room temperature while dielectric properties were investigated in a wide range of temperature (T = 25°C-550°C) and frequency (20Hz-1MHz).

Keywords: ceramics, Bi₅Ti₃FeO₁₅, Ho³⁺ doping, microstructure and structure, dielectric properties

1. Introduction

Bismuth layered perovskite-like oxides, i.e. Aurivillius phases represent a class of ferroelectric materials with wide potential applications, primarily for the construction of new information storage systems [1,2]. Nowadays, the Aurivillius phases have been considered an alternative to lead-containing perovskite materials [3]. The wide interest in layered perovskites grows up mainly due to the fact that they enable great possibilities in the selection of chemical composition, among others by isomorphic substitutions in positions A and B and without maintaining stoichiometry as a result of cationic or anionic vacancies. As a consequence of such substitution or lack of stoichiometry, the physical properties of the material vary widely [4,5].

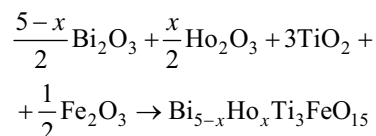
It is well known that, ceramics Bi₅Ti₃FeO₁₅ is the first member of the homologous series of Aurivillius compounds Bi_{m+1}Ti₃Fe_m3O_{3m+3} [6,7]. The pure Bi₅Ti₃FeO₁₅ possesses an orthorhombically distorted perovskite crystal structure with space group of A21am at room temperature. Ferroelectric Curie temperature (T_c) for Bi₅Ti₃FeO₁₅ was determined to be 1023 K corresponding to a structural transition from the A21am to the I4/mmm [8]. In addition, it was found that BTF favors the anti-ferromagnetic (AFM) ordering with its Neel point T_N of about 80 K [9,10].

In the literature it can be found a lot of information about pure Bi₅Ti₃FeO₁₅. The properties of rare earth metal doped Bi₅Ti₃FeO₁₅ ceramics are not well known.

The aim of this work was to fabricate Bi_{5-x}Ho_xTi₃FeO₁₅ ceramics by the conventional solid-state sintering method in the range of Ho concentration (x = 0 – 0.1). Then, the morphology, crystalline structure and dielectric properties of the obtained materials were studied. Enriching knowledge of structural and dielectric properties will create the opportunity to design innovative functional materials in the future.

2. Experiment

The appropriate amounts of reagent-grade oxide powders, viz. Bi₂O₃, Fe₂O₃, TiO₂ and Ho₂O₃ (all 99.9% purity) were thoroughly weighted according to the anticipated reaction:



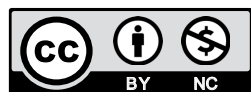
The constituent components were mixed using planetary ball mill for 24 h in ethyl alcohol medium. The powders were

¹ UNIVERSITY OF SILESIA, FACULTY OF SCIENCE AND TECHNOLOGY, INSTITUTE OF MATERIALS ENGINEERING, 12, ZYTANIA STR., 41-200 SOSNOWIEC, POLAND

² LUBLIN UNIVERSITY OF TECHNOLOGY, INSTITUTE OF ELECTRONICS AND INFORMATION TECHNOLOGY, 38A NADBYSTRZYCKA STR., 20-618 LUBLIN, POLAND

³ LUBLIN UNIVERSITY OF TECHNOLOGY, DEPARTMENT OF APPLIED PHYSICS, 36 NADBYSTRZYCKA STR., 20-618 LUBLIN, POLAND

* Corresponding author: jolanta.dzik@us.edu.pl



dreid and then the pellets were formed and pressed into discs with the diameter of 10 mm and 1mm thickness. The synthesis was carried out at $T = 750^{\circ}\text{C}$ in corundum crucible with air atmosphere for 10 h. After thermal treatment, the pellets were crushed in a mortar and the synthesized material was wet milled and dried again. The final sintering of the synthesized powder was carried out using following technological conditions: $T = 950^{\circ}\text{C}$, $t = 3$ h.

The microstructure was examined by a scanning electron microscope SEM, JSM-7100F TTL LV. For image analysis enabling microstructural classification of ceramics and several images from each sample were made. The procedure of registering sample images was based on the random selection of several fields distributed over the entire surface of the tested ceramics. The microanalysis system made it possible to perform both point: surface analysis of the chemical composition of the samples and linear distribution of elements in the material in question. The results were compared with the theoretical ones, and calculated on the basis of the general formula of $\text{Bi}_{5-x}\text{Ho}_x\text{Ti}_3\text{FeO}_{15}$ ceramics. The obtained results of measurements of the percentage content of individual elements are given as oxides.

The crystal structure of the obtained samples was investigated using Panalytical-Empeyan diffractometer with $\text{CuK}\alpha$ radiation. The diffractometer was working in the standard $\Theta - 2\theta$ mode in the 2θ range 10° - 90° and the step $\Delta 2\theta = 0.01^{\circ}$. The phase and structural analyses of the recorded XRD patterns were performed with an X'Pert HighScore Plus program.

Silver electrodes were deposited on BTFO ceramics by firing silver paste at temperature $T = 700^{\circ}\text{C}$ to form parallel plate measuring capacitor. The computerized automatic system based on precision LCR meter Agilent E4980A was used to measure the temperature dependencies of permittivity in a frequency range $\nu = 20$ Hz-1 MHz.

3. Results and discussion

Fig. 1 presents diffractograms registered for the studied samples. All the visible peaks were assigned to orthorhombic phase (space group Fmm2) characteristic of $\text{Bi}_5\text{Ti}_3\text{FeO}_{15}$ compound. No additional peaks were detected, thus it may be claimed that pure $\text{Bi}_{5-x}\text{Ho}_x\text{Ti}_3\text{FeO}_{15}$ solid solutions were obtained. That

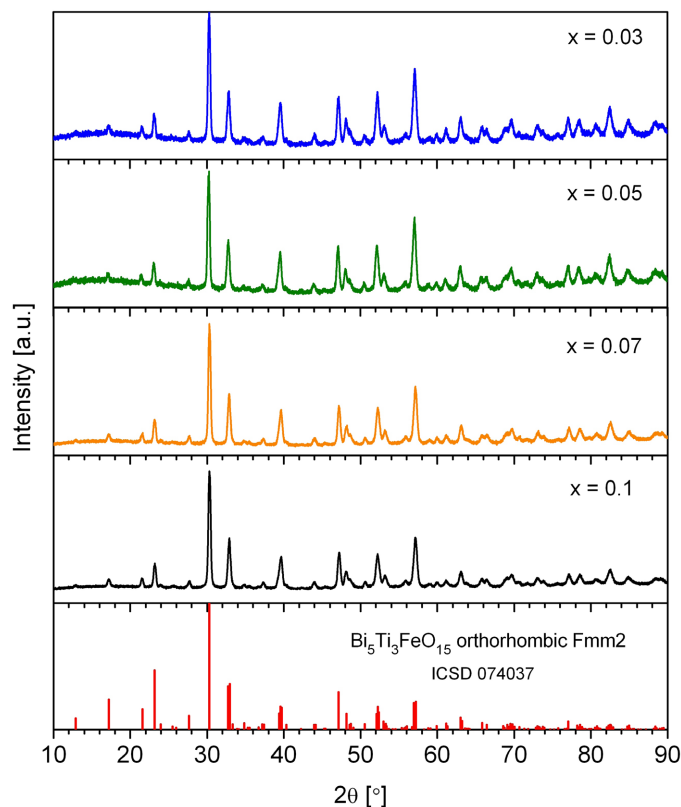


Fig. 1. X-ray diffraction patterns of BHTF solid solutions

TABLE 1

Structural parameters derived from XRD spectra analyses. The uncertainty of a and b parameters determination is range of 0.002 Å while the uncertainty of c parameter is less than 0.02 Å

	Crystal system	Space group	a [Å]	b [Å]	c [Å]	$\alpha = \beta = \gamma$ [°]	V [Å ³]
BTFO [12]	Orthorhombic	Fmm2	5.432	5.469	41.149	90	1222.4
BHTFO3	Orthorhombic	Fmm2	5.439	5.465	41.177	90	1223.9
BHTFO5			5.436	5.462	41.179	90	1222.6
BHTFO7			5.434	5.457	41.169	90	1220.7
BHTFO10			5.434	5.458	41.228	90	1222.7

TABLE 2

Theoretical and experimental content of elements (calculation for simple oxide) for BFT and BHTF ceramics

Formula	Oxide content by EDS measurement [%]				Theoretical content of oxides [%]				Content error [%]			
	Bi_2O_3	Fe_2O_3	TiO_2	Ho_2O_3	Bi_2O_3	Fe_2O_3	TiO_2	Ho_2O_3	Bi_2O_3	Fe_2O_3	TiO_2	Ho_2O_3
BTFO	7,750	0,560	1,690	—	7,848	0,538	1,614	—	0,786	3,975	4,583	—
BHTFO3	7,807	0,538	1,615	0,038	7,723	0,548	1,69	0,039	1,087	1,781	4,612	2,043
BHTFO5	7,781	0,539	1,616	0,064	7,680	0,560	1,694	0,066	1,303	3,957	4,812	3,549
BHTFO7	7,754	0,539	1,6177	0,089	7,674	0,56	1,68	0,086	1,038	3,895	3,884	3,680
BHTFO10	7,714	0,539	1,619	0,128	7,645	0,565	1,660	0,130	0,897	4,729	2,556	1,829

is to say, Ho element successfully substitutes the position of the Bi site. The positions of peaks agree well with the standard pattern indexed by 074037 ICSD card number shown in the bottom panel of Fig. 1.

Structural parameters derived from XRD spectra analyses were summarized in Tab. 1. It can be noted that the changes of lattice parameters and cell volume are almost within the range of the uncertainty of measurement. In particular, no structural transformation caused by Ho substitution was detected. Bai et al. [11] reported transformation from Fmm2 symmetry to $A2_1am$ caused by $x = 0.25$ substitution of Ho ions and proved by splitting of the peak at $2\theta = 30^\circ$. Thus, it may be concluded that doping with $x = 0.03 \div 0.1$ of Ho ions does not affect the structure of BTFO significantly.

The contents all of Bi, Ho, Ti and Fe elements obtained from EDS analysis were recalculated to the mass of the suitable oxides. The final content of the constituent oxides agrees well with the planned chemical composition. The discrepancy between theoretical composition and experimental content of elements is less than 4.8% what is consistent with the resolution of the utilized method of investigation.

SEM photographs showing morphology of fracture for BHTFO ceramics are presented in Fig. 2. These images reveal lamellar grains of different orientation, overlapping one another. Such morphology is characteristic of layer structures of the Aurivillius type. The pictures show that the admixture of holmium has a significant impact on the size of the grains. There is an evident decrease in grain size of Ho modified ceramics in comparison with pure BTFO. Increased holmium concentration causes a significant reduction in grain size. Yu Long Bai et al. [13] have found that the grain size reduction in holmium-doped materials can be interpreted by the suppression of oxygen vacancy concentration due to the charge compensation mechanism, which ultimately results in slower oxygen ion motion and consequently lower grain growth rate. This behaviour is typical for Aurivillius bismuth layered compounds due to the preferential growth of the ab crystalline plane. The rare-earth ions are known to suppress the grain growth in perovskites, which can be attributed to their lower diffusivity [9].

The measurements of electric permittivity versus temperature were carried out in an electric measuring field at frequencies in the range of 20 Hz-1 MHz. Temperature dependences of

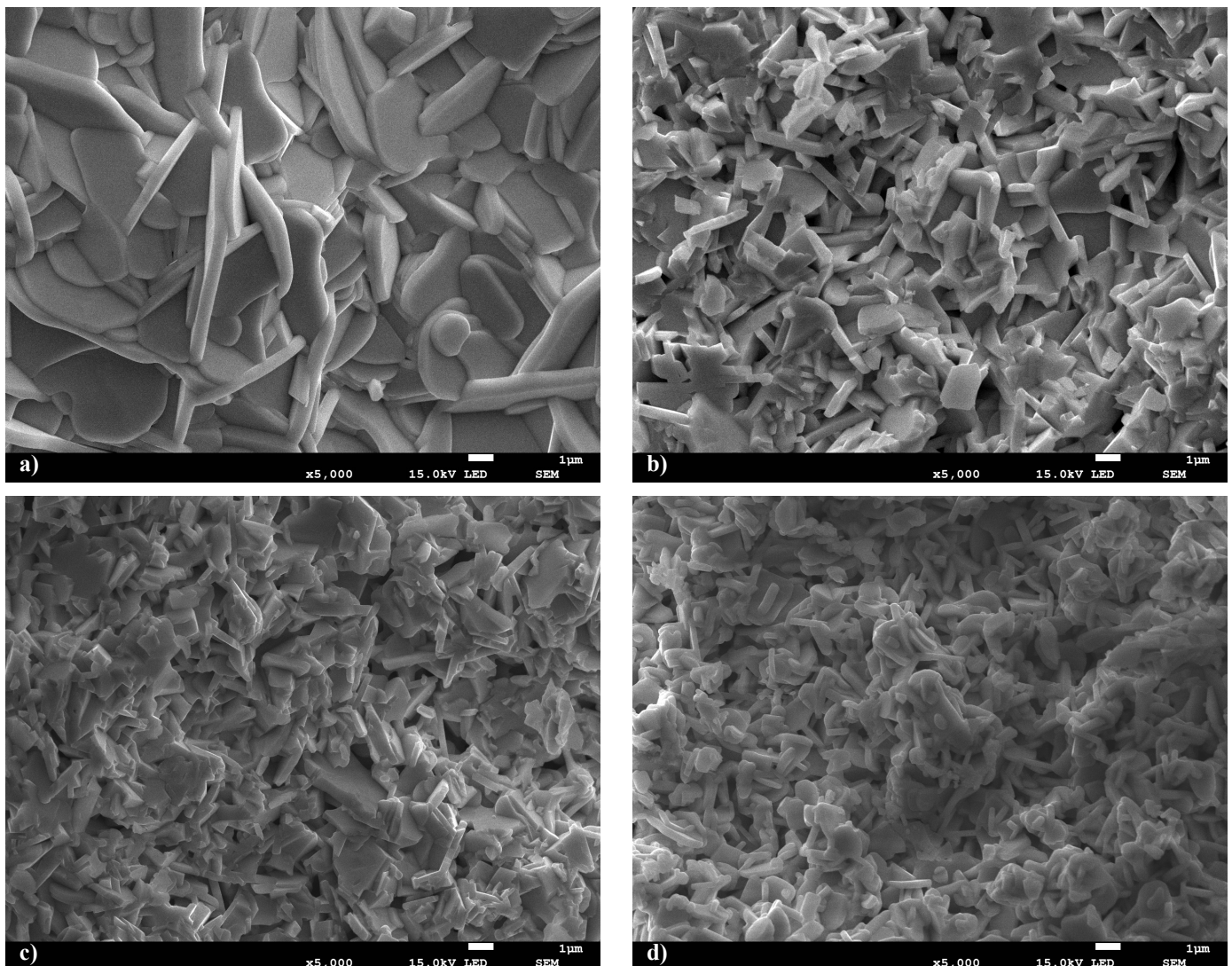


Fig. 2. SEM photographs of fracture for a) BHTFO3, b) BHTFO5, c) BHTFO7, d) BHTFO10 ceramics

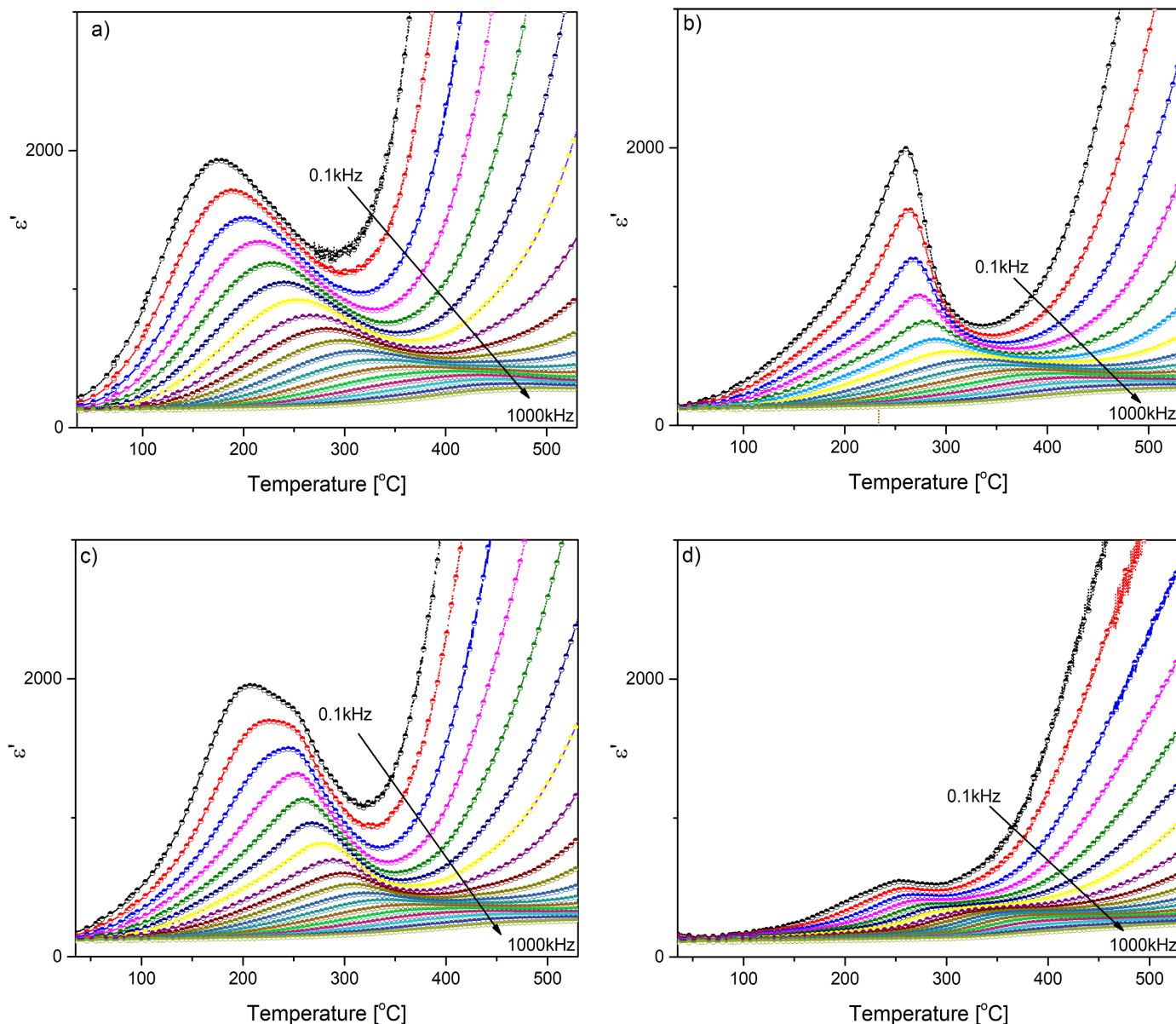


Fig. 3. Temperature dependencies of electric permittivity ϵ' for a) BHTFO3, b) BHTFO5, c) BHTFO7 and d) BHTFO10

the electric permittivity of all ceramics are presented in Fig. 3. It is evident that electric permittivity decreases. Also with frequency change the value of electric permittivity decreases, and the maximum curve $\epsilon'(T)$ shifts towards higher temperatures. While the frequency of the measuring field increases the curve of the dependence of the electric permittivity of ceramics shows frequency dispersion in wide range of the temperature ($T = 200\text{--}300^\circ\text{C}$). It is known, that the ferroelectric phase transition of BTFO at the temperature $T = 1023\text{ K}$ [8], which is out of the scope of the scale of the measurement temperature.

The dependence of electric permittivity on temperature shows the wide maximum which is characteristic of the materials of ion disorder or relaxing properties [14]. It can be found in literature that the relaxation properties and dipole disorder of the Aurivillius phases are associated with the stacking faults in the perovskite like-layers of the so-called Aurivillius mixed phases [15,16].

Fig. 4 shows the frequency dependence of the tangent of the dielectric loss angle on temperature for obtained ceramics.

The dielectric losses over the entire temperature range are similar for all the ceramics. The courses of the dependence of the tangent of the dielectric loss angle on the temperature $\text{tg}(\delta)$ show a sharp increase with increasing temperature.

4. Conclusions

Using the mixed oxide method followed by pressureless sintering, $\text{Bi}_{5-x}\text{Ho}_x\text{Ti}_3\text{FeO}_{15}$ ceramics were successfully fabricated from stoichiometric amount of Bi_2O_3 , TiO_2 , Ho_2O_3 and FeO_3 powders, via the solid-state reaction route. Such morphology is characteristic of layer structures of the Aurivillius type. XRD studies showed that hafnium doping for $x = 0.03 \div 0.1$ doesn't affect the structure of BFTO significantly. All peaks were as-

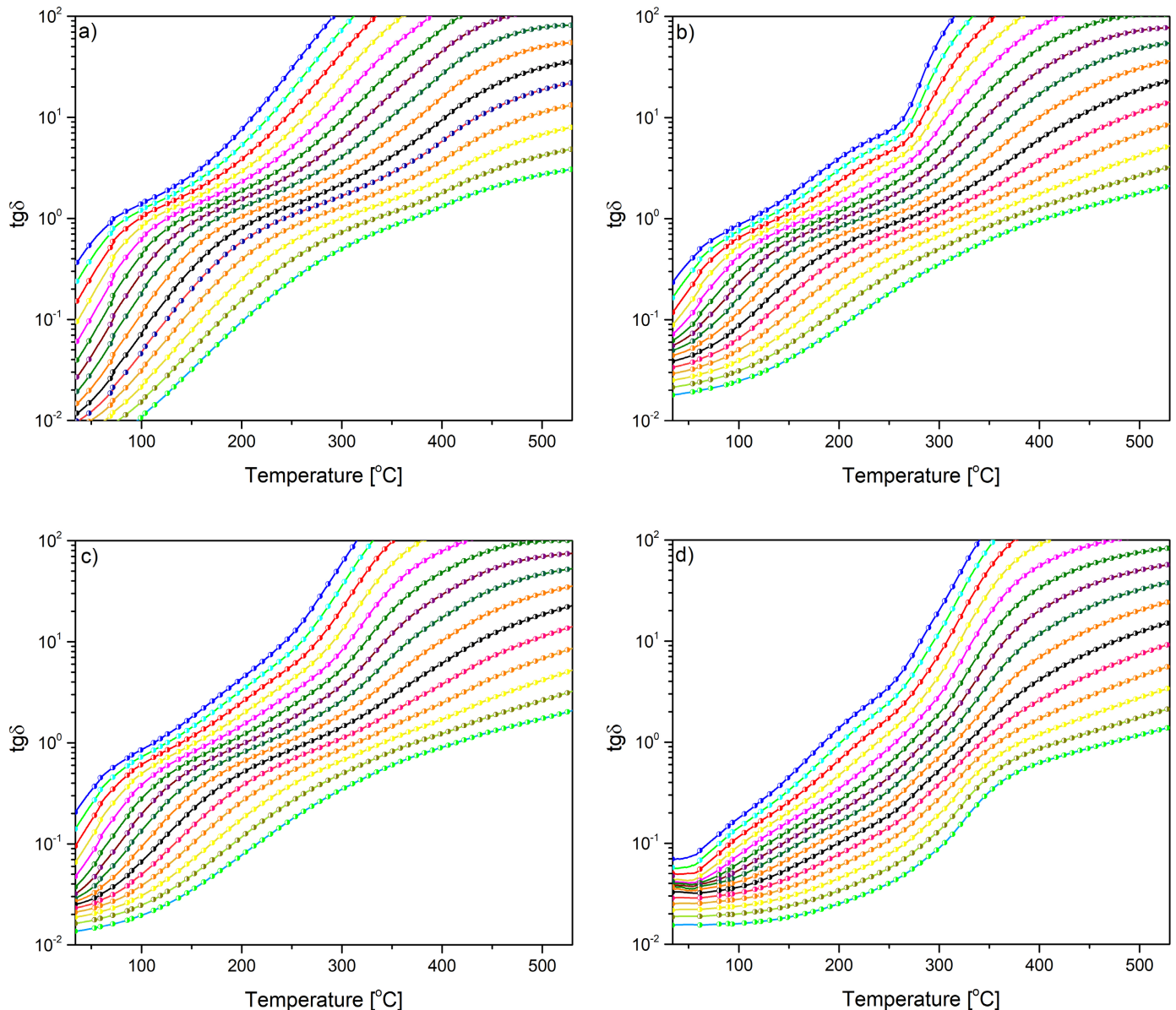


Fig. 4. Temperature dependencies of the tangent of dielectric losses $\tan\delta$ for a) BHTFO3, b) BHTFO5, c) BHTFO7 and d) BHTFO10

signed to orthorhombic phase (space group Fmm2) characteristic of $\text{Bi}_5\text{Ti}_3\text{FeO}_{15}$ compound. There is no evidence of the secondary phases or the formation of un-reacted Ho_2O_3 what confirms the complete incorporation of the Ho-ion in the $\text{Bi}_{5-x}\text{Ho}_x\text{Ti}_3\text{FeO}_{15}$ lattice. Electric permittivity decreases monotonically with increasing of temperature. The dependence of dielectric loss angle values on temperature $\text{tg}\delta(T)$ shows a sharp growth with increasing temperature.

REFERENCES

- [1] J.D. Bobic, R.M. Katiliute, M. Ivanov, M.M. Vijatovic' Petrovic, N.I. Ilic, A.S. Dzunuzovic, J. Banys, B.D. Stojanovic, Dielectric, ferroelectric and magnetic properties of La doped $\text{Bi}_5\text{Ti}_3\text{FeO}_{15}$ ceramics, *J. Mater. Sci.-Mater. El.* **2** (2015).
- [2] M. Wu, Z. Tian, Songliu Yuan, Zhengbei Huang, Magnetic and optical properties of the Aurivillius phase $\text{Bi}_5\text{Ti}_3\text{FeO}_{15}$, *Mater. Lett.* **68**, 190-192 (2012).
- [3] A. Moure, Review and Perspectives of Aurivillius Structures as a Lead-Free Piezoelectric System, *Appl. Scienc.* **7** (2003).
- [4] A. Lisińska-Czekaj, Wielofunkcyjne materiały ceramiczne na podstawie tytanianu bizmutu, Uniwersytet Śląski, Wydawnictwo Gnome, Katowice 2012.
- [5] X.Gao, L. Zhang, Chuanbin Wang, Q. Shen, Anisotropic electrical and magnetic properties in textured $\text{Bi}_5\text{Ti}_3\text{FeO}_{15}$ ceramics, *J. Eur. Ceram. Soc.* **37** (2017).
- [6] W. Bai, J.Y. Zhu, J.L. Wang, T. Lin, J. Yang, X.J. Meng, X.D. Tang, Z.Q. Zhu, J.H. Chu, Effects of annealing temperature on the structures, ferroelectric and magnetic properties of Aurivillius $\text{Bi}_5\text{Ti}_3\text{FeO}_{15}$ polycrystalline films, *J. Magn. Magn. Mater.* **324** (2012).

- [7] H. Sun, Y. Wu, T. Yao, Y. Lu, H. Shen, F. Huang, X. Chen, Electrical and magnetic properties of Aurivillius phase $\text{Bi}_5\text{Fe}_{1-x}\text{Ni}_x\text{Ti}_3\text{O}_{15}$ thin films prepared by chemical solution deposition, *J. Alloy Compd.* **765** (2018).
- [8] C.H. Hervoche, A. Snedden, R. Riggs, S.H. Kilcoyne, P. Manuel, P. Lightfoot, Structural Behavior of the Four-Layer Aurivillius-Phase Ferroelectrics $\text{SrBi}_4\text{Ti}_4\text{O}_{15}$ and $\text{Bi}_5\text{Ti}_3\text{FeO}_{15}$, *J. Solid State Chem.* **164** (2002).
- [9] J.D. Bobic, R.M. Katiliute, M. Ivanov, M.M. Vijatovic' Petrovic', N.I. Ilic', A.S. Dz'unuzovic', J. Bany, B.D. Stojanovic', Dielectric, ferroelectric and magnetic properties of La doped $\text{Bi}_5\text{Ti}_3\text{FeO}_{15}$ ceramics, *J. Mater. Sci.-Mater. El.* **27** (2016).
- [10] M. Wu, Z. Tian, Songliu Yuan, Z. Huang, Magnetic and optical properties of the Aurivillius phase $\text{Bi}_5\text{Ti}_3\text{FeO}_{15}$, *Mater. Lett.* **68** (2012).
- [11] Y. Bai, J. Chen, R. Tian, S. Zhao, Enhanced multiferroic and magnetoelectric properties of Ho, Mn co-doped $\text{Bi}_5\text{Ti}_3\text{FeO}_{15}$ films, *Mater. Lett.* **164** (2016).
- [12] F. Kubel, H. Schmid, X-ray room temperature structure from single crystal data, powder diffraction measurements and optical studies of the aurivillius phase $\text{Bi}_5(\text{Ti}_3\text{Fe})\text{O}_{15}$, *Ferroelectrics* **129** (1992).
- [13] Y. Bai, J. Chena, S. Zhao, Magnetoelectric fatigue of Ho-doped $\text{Bi}_5\text{Ti}_3\text{FeO}_{15}$ films under the action of bipolar electrical cycling, *RSC Advance* **47** (2016).
- [14] N.A. Lomanova, V.V. Gusarov, Electrical properties of perovskite-like compounds in the $\text{Bi}_2\text{O}_3\text{-Fe}_2\text{O}_3\text{-TiO}_2$ system, *Inorganic Materials* **47** (2011).
- [15] K. Uchino, S. Nomura, Critical exponents of the dielectric constants in diffused-phase-transition crystals, **44** (1982).
- [16] V.L. Morozov, V. Ugolkov, V. Gusarov, Properties of Aurivillius phases in the $\text{Bi}_4\text{Ti}_3\text{O}_{12}\text{-BiFeO}_3$ system, N.A. Lomanova, M.I., *Inorganic Materials* **42** (2006).